MOLECULAR ECOLOGY

Molecular Ecology (2016) doi: 10.1111/mec.13583

Transcontinental dispersal, ecological opportunity and origins of an adaptive radiation in the Neotropical catfish genus *Hypostomus* (Siluriformes: Loricariidae)

GABRIEL S. C. SILVA,*[1] FÁBIO F. ROXO,*[1] NATHAN K. LUJAN,†‡ VICTOR A. TAGLIACOLLO,§ CLAUDIO H. ZAWADZKI¶ and CLAUDIO OLIVEIRA*

Departamento de Morfologia, Laboratório de Biologia e Genética de Peixes, IB–UNESP, Campus de Botucatu, Botucatu, 18618–970 São Paulo, Brazil, †Center for Systematic Biology and Evolution, Academy of Natural Sciences of Drexel University, 1900 Benjamin Franklin Parkway, Philadelphia, PA 19103, USA, ‡Department of Biology, University of Toronto Scarborough, Toronto, ON M1C1A4, Canada, §Programa de Pós Graduação Ciências do Ambiente (CIAMB), Universidade Federal do Tocantins, Palmas, Tocantins 77001–090, Brazil, ¶Departamento de Biologia, Núcleo de Pesquisas em Limnologia, Ictiologia e Aquicultura (Nupélia), Universidade Estadual de Maringá, Maringá, 87020–900, Paraná, Brazil

Abstract

Ecological opportunity is often proposed as a driver of accelerated diversification, but evidence has been largely derived from either contemporary island radiations or the fossil record. Here, we investigate the potential influence of ecological opportunity on a transcontinental radiation of South American freshwater fishes. We generate a species-dense, time-calibrated molecular phylogeny for the suckermouth armored catfish subfamily Hypostominae, with a focus on the species-rich and geographically widespread genus *Hypostomus*. We use the resulting chronogram to estimate ancestral geographical ranges, infer historical rates of cladogenesis and diversification in habitat and body size and shape, and test the hypothesis that invasions of previously unoccupied river drainages accelerated evolution and contributed to adaptive radiation. Both the subfamily Hypostominae and the included genus *Hypostomus* originated in the Amazon/Orinoco ecoregion. *Hypostomus* subsequently dispersed throughout tropical South America east of the Andes Mountains. Consequent to invasion of the peripheral, low-diversity Paraná River basin in southeastern Brazil approximately 12.5 Mya, Paraná lineages of *Hypostomus*, experienced increased rates of cladogenesis and ecological and morphological diversification. Contemporary lineages of Paraná *Hypostomus* are less species rich but more phenotypically diverse than their congeners elsewhere. Accelerated speciation and morphological diversification rates within Paraná basin *Hypostomus* are consistent with adaptive radiation. The geographical remoteness of the Paraná River basin, its recent history of marine incursion, and its continuing exclusion of many species that are widespread in other tropical South American rivers suggest that ecological opportunity played an important role in facilitating the observed accelerations in diversification.

Keywords: freshwater fish, geodispersal, macroevolution, molecular evolution, systematics

Received 17 August 2015; revision received 29 January 2016; accepted 3 February 2016

Introduction

A central aim of evolutionary biology is to understand why species richness and phenotypic diversity are unevenly distributed across the tree of life (Stanley

Correspondence: Fábio F. Roxo, Fax: + 14 38116264 120; E-mail: roxoff@hotmail.com.br

[1]These authors contributed equally to this work.

1998; Mace *et al.* 2003; Venditti *et al.* 2010; Rabosky *et al.* 2012). Life is replete with examples of both 'explosive radiations' – characterized by rapid diversification into staggering numbers of species and phenotypes (e.g. African cichlid fishes, Caribbean *Anolis* lizards, Hawaiian silversword plants) – and 'living fossil' lineages – characterized by low species richness and morphological stasis for much of their evolutionary history (e.g. lungfishes, tuatara, *Equisetum*; Rabosky *et al.* 2013). Causes for such disparity can be broadly divided into mechanisms that accelerate speciation and/or phenotypic diversification rates (e.g. adaptive radiation, mimicry rings) and those that require no differences in underlying rates (e.g. differences in clade age or extinction rate). Only recently, with the advent of low-cost, fast and comprehensive molecular data (e.g. Boubli *et al.* 2012; Rabosky *et al.* 2012; Sorenson *et al.* 2014) and a growing plethora of comparative statistical techniques (e.g. Ricklefs 2007; Alfaro *et al.* 2009; Paradis 2011; Revell 2012; Rabosky 2014) have both robust phylogenies and techniques for identifying potential mechanisms been available to biologists. A major current goal to link results of these evolutionary models to climatic and geophysical processes to understand how large-scale Earth processes influence biological diversification.

Broadly distributed radiations of freshwater fishes are excellent systems in which to investigate linkages between biological diversification and geomorphological processes that shape the Earth's surface. Freshwater fishes are highly diverse, and most are entirely restricted to freshwater habitats. Moreover, physical connections and slopes between and within these habitats shift in response to geomorphic processes. Phylogenies of freshwater fishes often reflect these events (Smith 1981; Hocutt & Wiley 1986; Mayden 1988; Lundberg *et al.* 1998; Cardoso *et al.* 2012; Lujan *et al.* 2015a; Tagliacollo *et al.* 2015). Indeed, geomorphological processes involving both the division of previously contiguous populations and the passive geodispersal of species between drainages have been linked to freshwater fish speciation and diversification both theoretically and empirically (Grant *et al.* 2007; Muneepeerakul *et al.* 2008; Winemiller *et al.* 2008; Bertuzzo *et al.* 2009; Albert & Crampton 2010).

When an evolutionary lineage reaches a new environment, such as an island or drainage basin that lacks similar species, it may gain access to ecological opportunities that promote diversification by relaxing selection on ecologically important traits (Ehrlich & Raven 1964; Yoder *et al.* 2010). In some noteworthy instances, this leads to adaptive radiation in which a clade displays accelerated diversification rates, correlation between ecological and phenotypic traits, and newly derived traits that permit increased performance (Schluter 2000). Although causal connections between ecological opportunity and biological diversification are often difficult to establish and differentiate from other drivers, macroevolutionary evidence for ecological opportunity's importance is strong. First, long-term decreases in rates of lineage and morphological diversification are common in many lineages throughout the fossil and extant biological record (Soltis *et al.* 2002; Mahler *et al.* 2010). Such decreases are primarily attributed to the saturation of niche space – that is the decline of ecological opportunity due to increasing exploitation – that is an expected consequence of species accumulation (Simpson 1949, 1953). Second, fossil and molecular data for some groups (e.g. trilobites, Hallam & Wignall 1997; mammals, Meredith *et al.* 2011) suggest that speciation rates have increased following mass extinctions – that is periods of increased ecological opportunity due to niche vacancies (Sepkoski 1981, 1998, 2002; Erwin *et al.* 1987; Erwin 2001).

In addition to these macroevolutionary patterns, theory predicts a number of shorter-term, population-level, ecological and physiological responses to increased ecological opportunity. For example, after a lineage reaches a new environment, its population may increase, it may occupy a broader range of microhabitats, and it may display a broader range of morphological or behavioural characteristics as a result of decreased competitive pressure (Crowell 1962; Losos & de Queiroz 1997). Easier access to new or alternative resources created by ecological opportunity should effectively flatten the adaptive landscape, making a wider range of phenotypes viable (Roughgarden 1972; Travis 1989; Lathi *et al.* 2009). This is supported by empirical studies of populations that show a broader range of phenotypes following release from predation, competition or other sources of stabilizing selection (Roughgarden 1972; Houle *et al.* 1994). Access to the extrinsic opportunities and mechanisms that are linked to invasion of a new environment are often dependent upon intrinsic aspects of a species' life history (e.g. vagility, fecundity, body size, ecological tolerance). Vagile species are more likely to invade a new habitat than philopatric species, and eurytopic species, which exhibit broad physiological and habitat tolerances, are more likely to succeed in a new habitat (Vrba 1980; Ribbink 1994).

Hypostominae is a species-rich (*c.* 447 valid species and 38 genera; Eschmeyer & Fong 2015) and monophyletic (Lujan *et al.* 2015b) group of primarily herbivorous and detritivorous catfishes restricted to the freshwaters of tropical Central and South America. Despite being broadly constrained to the primary consumer niche, Hypostominae lineages are known to display a wide range of jaw morphologies consistent with their fine-scale partitioning of basal food resources

including algae, detritus and wood (Lujan *et al.* 2011, 2012; Lujan & Armbruster 2012). Containing approximately 141, or about 30%, of all valid Hypostominae species, *Hypostomus* is the most species-rich genus in the subfamily and is among the most common and ubiquitous fish genera throughout the continental freshwaters of tropical South America. Our goal in this study was to examine the hypothesis that geographical dispersal via landscape-scale geomorphological events has accelerated rates of diversification of lineages (cladogenesis), maximum body size (MBS), and body shape within Hypostominae, particularly in the genus *Hypostomus*. We do this by (i) generating a species-dense, time-calibrated phylogeny for Hypostominae with a focus on *Hypostomus*, (ii) using the obtained chronogram to estimate ancestral geographical ranges and (iii) infer historical diversification rates in occupied habitat, body size and body shape.

Material and methods

Taxon sampling

Our objective in taxonomic sampling was to comprehensively sample genera within Hypostominae (*sensu* Lujan *et al.* 2015b) and to maximize the breadth of genera representing other loricariid subfamilies and tribes. Our in-group (Hypostominae) included 124 specimens spanning 24 genera and four to five tribes (*sensu* Lujan *et al.* 2015b). To test for monophyly of Hypostominae, we compiled a broad range of outgroups representing all other subfamilies of Loricariidae plus Astroblepidae and Callichthyidae. Specimens sequenced for this study are listed in Tables S1 and S2 (Supporting information). Sequence data for many taxa outside the Hypostominae, including members of the subfamilies Loricariinae, Hypoptopomatinae and Rhinelepinae, were obtained from previously published studies (Montoya-Burgos *et al.* 1998; Chiachio *et al.* 2008; Covain & Fisch-Muller 2012; Roxo *et al.* 2012, 2014) via the GenBank database.

Members of two other Loricarioidei families (Astroblepidae: *Astroblepus* sp. and Callichthyidae: *Hoplosternum littorale*, *Corydoras imitator* and *C. oiapoquensis*) were selected as outgroups based on relationships established in previous larger-scale phylogenetic analyses of both morphological (de Pinna 1993, 1998) and molecular (Sullivan *et al.* 2006) data. Vouchers of all sequenced samples were deposited in the Auburn University Natural History Museum, Auburn, Alabama, USA (AUM); Laboratório de Biologia e Genética de Peixes, Departamento de Morfologia, Instituto de Biociências, Universidade Estadual Paulista, Botucatu, São Paulo, Brasil (LBP); the Núcleo de Pesquisas em Limnologia, Ictiologia e Aquicultura, Universidade Estadual de Maringá, Paraná, Brasil (NUP); Museum d'Histoire Naturelle, Département d'Herpétologie et Ichthyologie, Ville de Genève, Genève, Switzerland (MHNG); or at the Smithsonian Tropical Research Institute, Balboa, Ancón, Panama (STRI). Specimens were identified directly by the authors GSCS and CHZ, except in the case of GenBank identifications, which were not changed.

DNA extraction and sequencing

Whole-genomic DNA was extracted from muscle, fin or liver samples preserved in 95% ethanol using the Wizard Genomic DNA Purification Kit (Promega, Madison, WI, USA). Partial sequences of the 16S rRNA, cytochrome *b* (cyt *b*) and F-reticulon 4 (RTN4) genes were amplified by polymerase chain reaction (PCR; primers listed in Table S3, Supporting information). Amplifications were performed in a total volume of 12.5 μL with 1.25 μL of 10× buffer (10 mM Tris-HCl+15 mM $MgCl_2$), 0.5 μL dNTPs (200 nM of each), 0.5 μL of each 5 mM primer, 0.05 μL Platinum® *Taq* Polymerase (LTI: Life Technologies Inc., Carlsbad, CA, USA), 1 μL template DNA (approximately 12 ng) and 8.7 μL ddH_2O. PCRs consisted of 30–40 cycles of 30 s at 95 °C, 15–30 s at 48–58 °C and 45–90 s at 72 °C (annealing temperature and duration depended on primers and species, Table S3, Supporting information). Nested PCRs were used to amplify the nuclear marker RTN4; the first amplification was performed using the primers Freticul4-D and Freticul4-R with a total volume of 12.5 μL for 30–40 cycles (30 s at 95 °C, 30 s at 48 °C and 135 s at 72 °C); and the second amplification was performed using the primers Freticul4 D2 and Freticul4 R2 with a total volume of 12.5 μL for 30–40 cycles (30 s at 95 °C, 30 s at 53–54 °C and 135 s at 72 °C). All PCR products were first visually identified on a 1% agarose gel and then purified using ExoSap-IT® (USB Corporation, Cleveland, OH, USA) following manufacturers' instructions. Purified PCR products were sequenced using the Big Dye® Terminator v3.1 Cycle Sequencing Ready Reaction Kit (ABI: Applied Biosystems Inc., Foster, CA, USA), purified again by ethanol precipitation and sequenced on a 3130 Genetic Analyzer (ABI) in the Instituto de Biociências, Universidade Estadual Paulista, Botucatu, São Paulo State.

Sequence alignment and phylogenetic inference

Two intronic regions of the RTN4 gene, totalling 63% of total locus length, were amplified and sequenced by our primers. All loci, including the entire RTN4 sequence, were first aligned using the MUSCLE algorithm (default parameters; Edgar 2004) followed by visual inspection and correction of the alignment requiring

almost no changes in base position. The total matrix consisted of 157 individuals × 3433 base pairs, or a total of approximately 548 800 characters, of which 40% were missing data. To detect potential sequencing errors due to contamination or paralogy, alignments for each gene were separately analysed by maximum likelihood (ML; Stamatakis *et al.* 2008) using the web server RAXML BLACKBOX (Stamatakis 2006). Sequences that resulted in obviously misplaced taxa in resulting gene trees were resequenced or eliminated from subsequent analyses. Because terminal redundancy can affect results of biogeographical analyses using dispersal–extinction–cladogenesis (DEC) models, we trimmed our final data set to include only one individual of each species.

We estimated the index of substitution saturation (Iss) and rates of transitions/transversions for each gene separately in DAMBE 5.2.31 (Xia & Xie 2001), as described by Xia *et al.* (2003) and Xia & Lemey (2009). Iss was estimated without considering gaps because unresolved sites reduce the ability of the method to test for phylogenetic signal. The best-fit partitioning scheme and nucleotide substitution model for each partition were determined using the greedy algorithm in the software PARTITIONFINDER (Lanfear *et al.* 2012), which was programmed to use PHYML to estimate likelihoods and the Akaike information criterion with correction for finite sample sizes (AICc) to choose the best model.

Maximum-likelihood (ML) analyses (Stamatakis *et al.* 2008) were performed using RAXML on the CIPRES Science Gateway computing cluster (Miller *et al.* 2010). RAXML implements a fast algorithm of heuristic searches using bootstrap (BS) resampling (Felsenstein 1985). Support for individual nodes was assessed using random start trees, the GTR+G model for all partitions of the matrix as determined by the software PARTITIONFINDER (Lanfear *et al.* 2012; Table S4, Supporting information), and independent ML tree searches consisting of 1000 pseudoreplicates each with all other parameters set to default values.

Bayesian inference (BI; Huelsenbeck & Ronquist 2001) was used to determine statistical support for alternative tree topologies through the estimation of posterior probabilities using the software MRBAYES v3.2.2 (Ronquist *et al.* 2012). This was made under different models for each partition of the matrix as determined by the software PARTITIONFINDER (Table S4, Supporting information), using a random tree to start the Markov chain Monte Carlo searches, and a duplex of four chains (nchains = 4) set to run simultaneously for 10 million generations, sampling tree space every 500th generation. This analysis was performed twice to ensure similarity of converged trees. Log-likelihood scores were calculated using the program TRACER 1.5 (Rambaut & Drummond 2007a) to determine whether independent searches of tree space had achieved stationarity based on their convergence within a stable – Ln range of values and effective sample sizes (ESS) exceeding 200. All sampled topologies beneath the asymptote (40%) were discarded as burn-in, and remaining trees were used to construct a 50% majority-rule consensus tree in TREEANNOTATOR v1.7.5 (Rambaut & Drummond 2007b).

Tree topology tests

Alternative tree topologies hypothesized by Lujan *et al.* (2015a,b) were evaluated in the program TREEFINDER (Jobb *et al.* 2004) using the Shimodaira and Hasegawa (SH) test (Shimodaira & Hasegawa 1999), the Approximately Unbiased (AU) test (Shimodaira 2002) and the Expected Likelihood Weights (ELW) method (Strimmer & Rambaut 2002). All tests were conducted under ML with the same 12-partition model as implemented in the RAXML analysis (Table S4, Supporting information).

Time calibration

The uncorrelated relaxed molecular clock (log-normal) was estimated using BEAST v1.7.5. (Drummond & Rambaut 2007). We used a clade-based approach that included each Hypostominae lineage in our analysis. The GTR+G model was used for all partitions (Table S4, Supporting information). The calibration prior was implemented using a log-normal distribution offset to 55 Mya with a mean and standard deviation of 1 for the origin of the genus *Corydoras* lineage (node including all Callichthyidae: *Corydoras imitator*, *C. oiapoquensis* and *Hoplosternum littorale*). The oldest known loricarioid fossil, *Corydoras revelatus* Cockerell (1925), was dated by Marshall *et al.* (1997) as Paleocene, which we used to assign a 55 My minimum age for the family Callichthyidae. We used a birth–death model for speciation likelihood and a starting tree obtained from ML. The analysis was run for 10 million generations and sampled every 1000th generation. Stationary and sufficient mixing of parameters (ESS > 200) was checked using TRACER v1.5 (Rambaut & Drummond 2007a). A consensus tree was built using TREEANNOTATOR v1.7.5 (Rambaut & Drummond 2007b).

Ancestral area estimation

Data on the geographical distributions of species in the Hypostominae were taken from the original species descriptions and information available from the online Catalog of Fishes (Eschmeyer & Fong 2015). To maintain consistency with previous biogeographical analyses of the subfamily Hypoptopomatinae (*sensu* Lujan *et al.*

2015b) by Chiachio *et al.* (2008) and Roxo *et al.* (2014), we assigned taxa to geographical areas using the ecoregion classification of Vari (1998), which was derived from patterns of endemism in the Neotropical endemic characiform family Curimatidae. Our samples were drawn from the following six of Vari's (1998) ecoregions: (i) Atlantic Coastal drainages, (ii) upper Paraná basin, (ii) Paraguay, lower Paraná and Uruguay basins, (iv) Amazon and Orinoco basins, (v) São Francisco basin and Northeastern Brazilian drainages and (vi) Pacific Coastal drainages and Magdalena basin.

Maximum-likelihood inference of geographical range evolution was performed using the dispersal–extinction–cladogenesis (DEC) model as implemented in LAGRANGE v2.0 (Ree *et al.* 2005; Ree & Smith 2008). Four DEC models were tested to estimate distribution ranges inherited by descending lineages at each node of the tree. Each model differed in the rates of dispersal between adjacent vs. nonadjacent areas (see Table S5, Supporting information for likelihood values and dispersal rates for each model). Model 3 (M3), which constrained dispersal rates between adjacent areas at 0.5 and areas separated by one or more intervening areas at 0.0001, obtained the highest ML values.

Speciation rates

We used BAMM version 2.1.0 (Rabosky 2014) to estimate speciation and extinction rates across the Hypostominae phylogeny. We assessed the effects of missing taxa on our tree by counting missing species for each lineage of our phylogeny (see Table S2, Supporting information for summary of missing genera and species). The analysis was conducted with two chains running simultaneously for a total of 5 million generations and tree space being sampled every 1000th generation. We used a burn-in value of 0.5 and checked for MCMC convergence using the BAMMTOOLS package (Rabosky *et al.* 2014) in the R statistical environment (R Core Team 2014) to plot log-likelihood values. To account for effects of phylogenetic uncertainty on our analyses, we conducted BAMM analyses of species diversification across 2500 trees sampled from the posterior distribution of topologies and branch lengths. To visualize the evolutionary rate dynamics from BAMM output results, we also used BAMMTOOLS.

Morphometric data

We measured 33 morphometric characters (doi: 10.5061/dryad.c8q11) on the bodies of two adult specimens from each of 124 specimens and 24 genera of Hypostominae, using 31 homologous landmarks originally proposed by Armbruster (2003a): 14 on the head, five on the mouth and the remainder on the trunk or fins. Although the suite of measurements we used was originally intended to maximize homology and taxonomic discrimination (Armbruster 2003a), many of the measurements are known to be functional, ecological correlates (e.g. mouth width, tooth row length, eye size, eye position, body depth, fin size; Gatz 1979; Winemiller 1991; Lujan & Armbruster 2012). All analyses described later are based on means of log-transformed trait values computed for each species. To remove the influence of body size on morphometric data, we used the program PAST v1.28 (Hammer *et al.* 2004) to normalize two coordinate dimensions, to divide all coordinate values by the centroid size for each specimen and to conduct a Procrustes fitting of the left half to a mirrored version of the right half (Dryden & Mardia 1998). We conducted a principal component analysis (PCA) using the covariance matrix of phylogenetically corrected residuals from the Past output. The first principal component (PC1) in the matrix of residuals accounted for 27.5% of variance in body shape for Hypostominae (values used for BAMM and phylomorphospace analyses) and 22.4% for *Hypostomus* (values used for an independent phylomorphospace analysis). PCA loadings are presented in Table S6 (Supporting information).

Diversification rates

We used BAMM version 2.1.0 (Rabosky 2014) to estimate rates of continuous trait evolution in body shape and maximum body size (MBS) values across the Hypostominae phylogeny. These analyses were conducted with two chains running simultaneously for a total of 50 million generations, with tree space sampled every 5000th generation. We used a burn-in value of 0.5 and checked for MCMC convergence using the BAMMTOOLS package in R (Rabosky *et al.* 2014). We conducted BAMM analyses of phenotypic evolution across 5000 trees sampled from the posterior distribution and visualized the evolutionary rate dynamics from BAMM output using BAMMTOOLS.

Habitat data and ancestral state estimation

Each Hypostominae species was classified according to one or more of the following five habitat categories (from Albert *et al.* 2011) based on original species descriptions, the online Catalog of Fishes (Eschmeyer & Fong 2015) and the authors' personal field experience: channels, rapids, streams, and low or high altitudes (see Table S2, Supporting information for habitat classifications and values for each species). Habitats for each species were coded using five binary (presence/absence) values, and the resulting matrix was examined in 1000 stochastic character map simulations using Simmap (Bollback 2006) in R (R Core Team 2014).

Phylomorphospace analysis

We generated two phylomorphospace biplots (Sidlauskas 2008) using the 'phylomorphospace' function in the PHYTOOLS v0.3-10 (Revell 2012) package in R (R Core Team 2014): one for all Hypostominae species and the second for only the genus *Hypostomus*. For each plot, the first principal component of size-corrected body shape for each taxonomic grouping was plotted against log maximum body size (MBS). Species colours in both plots correspond to ecoregion colour in the ancestral area estimation. In the Hypostominae plot, a convex hull was drawn around all *Hypostomus* species, and in the *Hypostomus* plot, a convex hull was drawn around all species from the Paraná River basin.

Results

DNA sequence alignment and substitution rates

The concatenated alignment of sequence data for 16S rRNA, cyt *b* and RTN4 genes resulted in a matrix consisting 3433 base pairs (bp); 971 bp was conserved and 2283 was variable. We found no evidence for saturation: the Iss.c value was greater than the Iss value (Xia *et al.* 2003; Xia & Lemey 2009), and the determination coefficients of transitions and transversions vs. genetic distance were higher than 0.7 (transitions $R^2 = 0.94$; transversions $R^2 = 0.98$). The observed transition/transversion ratio was 1.9, with nucleotide frequencies of 25.7% for adenine, 29.2% for thymine/uracil, 26.9% for cytosine and 18.1% for guanine.

Phylogenetic relationships

Within Hypostominae, our results (Fig. S1–S4, Supporting information) supported monophyly of six of the nine tribe-level clades identified by Lujan *et al.* (2015b): the *Chaetostoma* Clade (BS = 99, PP = 1), the '*Pseudancistrus*' Clade (BS = 91, PP = 1), Ancistrini (BS = 50), the *Pseudancistrus* Clade (BS = 97, PP = 1), the *Peckoltia* clade (BS = 92, PP = 1) and Hypostomini (BS = 99, PP = 1; see Figs S1–S4, Supporting information). One of Lujan *et al.*'s (2015b) tribe level clades was not examined (the *Lithoxus* Clade, consisting of nine small species restricted to the Guiana Shield), and two tribe level clades from that study were not supported as monophyletic: Monophyly of the *Hemiancistrus* Clade, containing the genus *Panaque* (BS = 100, PP = 1) and a clade of four other genera (*Baryancistrus*, *Hemiancistrus*, *Parancistrus* and *Spectracanthicus*; BS = 65), was not supported. Also, monophyly of the *Acanthicus* Clade, containing our *Leporacanthicus* clade (BS = 99, PP = 1) and *Megalancistrus* clade (BS = 100, PP = 1), was not supported. However, a topology test did not reject the hypothesis of monophyly of Lujan *et al.*'s (2015b) *Acanthicus* Clade (i.e. *Megalancistrus* being sister to *Leporacanthicus* + *Pseudacanthicus*). See Table S7 (Supporting information) for results of our topology tests.

Relaxed clock and ancestral area estimation

The mean substitution rate across all loci estimated using BEAST was 0.29% per My. The subfamily Hypostominae was estimated by BEAST to have originated during the Eocene approximately 43.1 Mya (26.3–67.2 Mya 95% HPD; see Fig. 1 for molecular clock tree including outgroups) and inferred by Lagrange to have originated in the Amazon/Orinoco ecoregion (Region D). Modern Hypostominae species are distributed across all six ecoregions in Fig. 1.

The ancestor of all tribe Hypostomini genera in our analysis was also hypothesized to have originated in the Amazon/Orinoco ecoregion approximately 15.1 Mya (8.5–23.6 Mya 95% HPD), as was the genus *Hypostomus*. *Hypostomus* was hypothesized to have reached the upper Paraná basin (Region B) approximately 12.5 Mya (7.2–19.2 Mya 95% HPD). All together, ancestral *Hypostomus* lineages were hypothesized to have dispersed into new drainages several times from 12.5 Mya to the present (see Fig. 1 for all dispersal events), resulting in their modern distribution across all but two of the ecoregions in Fig. 1 (i.e. samples missing only from Region E: São Francisco basin plus Northeastern Brazilian drainages, and Region F: Pacific Coastal drainages plus Magdalena basin).

Speciation rates

The mean phylorate plot for speciation suggests that the tribe Hypostomini experienced consistently higher cladogenesis rates than any other lineage within Hypostominae (Fig. 2). Within Hypostomini, speciation rates were highest in the genus *Hypostomus*. Moreover, the consensus phylorate plot and marginal probabilities of rate shifts plot support shifts in speciation rate at the node and along the branch (respectively) giving rise to *Hypostomus*. Our speciation rate-through-time plot suggests that speciation rates throughout Hypostominae began a steady increase approximately 15 Mya, coincident with the origin of the genus *Hypostomus* (Fig. 2).

Morphometric diversification rates

The mean phylorate plot for morphometric diversification (Fig. 3) suggests that the tribe Hypostomini

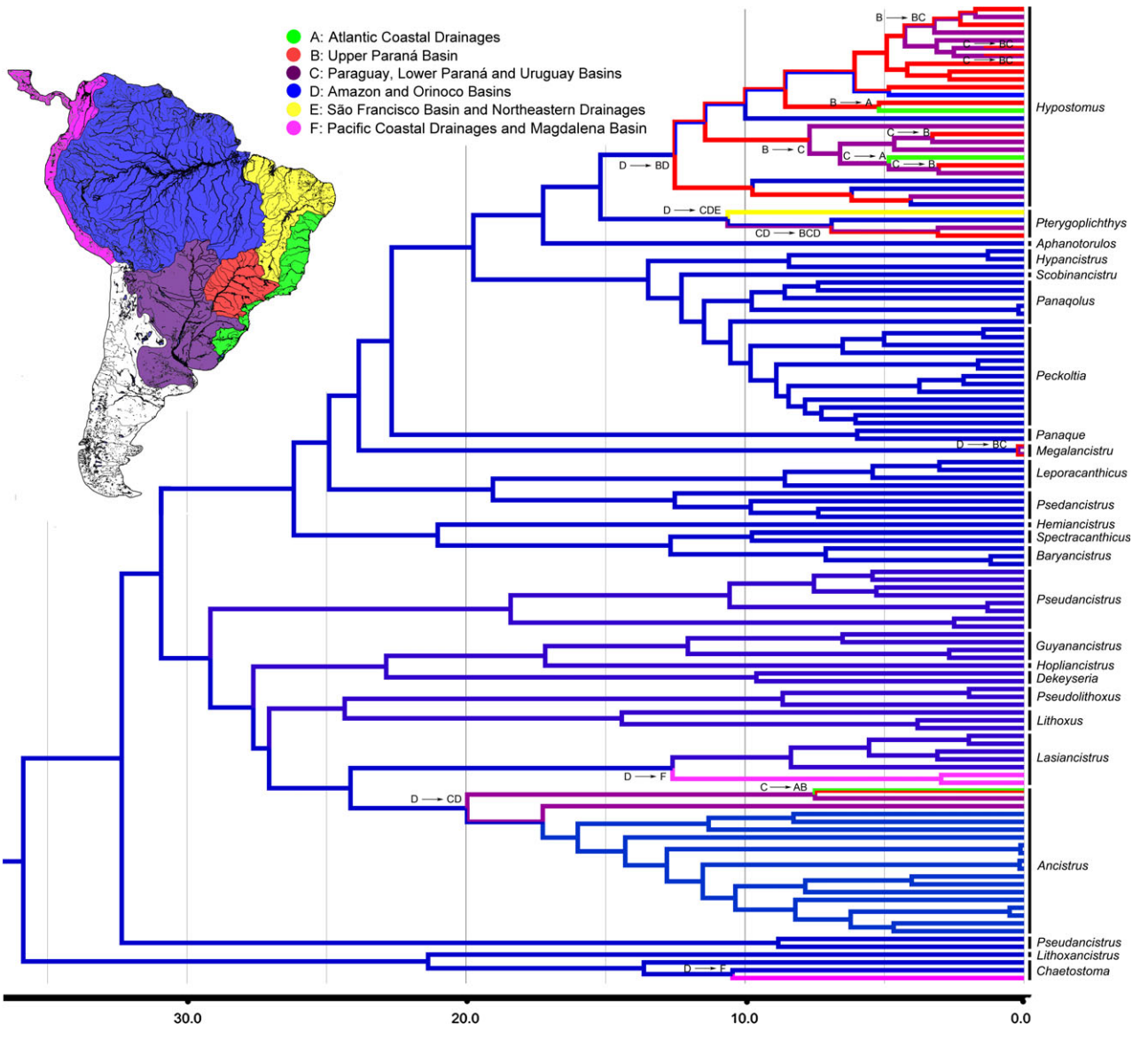

Fig. 1 Time-calibrated phylogeny for the loricariid catfish subfamily Hypostominae, illustrating ancestral range estimation and species range expansion through time. The chronogram was calibrated with a log-normal distribution offset to 55 Mya with a mean and standard deviation of 1 for the origin of the node including all Callichthyidae (*Corydoras imitator*, *C. oiapoquensis* and *Hoplosternum littorale*). The maximum-likelihood inference of geographical range evolution was performed using a dispersal–extinction–cladogenesis (DEC) model. The order of taxa in the phylogeny follows the order in Table S1–S2 and Figs S1–S4 (Supporting information).

experienced elevated rates of body shape diversification throughout its evolution, with highest rates observed along branches leading to members of the genus *Hypostomus*. Moreover, marginal probabilities of shifts in body shape diversification show high probabilities of shifts within the tribe Hypostomini, with shifts concentrated within *Hypostomus* (Fig. 3). The trait rate-through-time plot indicates that overall rates of Hypostominae body shape diversification increased slightly and steadily until approximately 5 Mya.

Body size diversification rates

Evolutionary rates of change in log maximum body size (MBS) were highest in a clade that included a diverse assemblage of Hypostominae genera (*Aphanotorulus*, *Hypancistrus*, *Hypostomus*, *Leporacanthicus*, *Megalancistrus*, *Panaqolus*, *Panaque*, *Peckoltia*, *Pterygoplichthys* and *Scobinancistrus*). Plots for both the consensus phylorate and marginal shift probabilities support a shift in body size diversification rate at the node giving rise to these genera (Fig. 4).

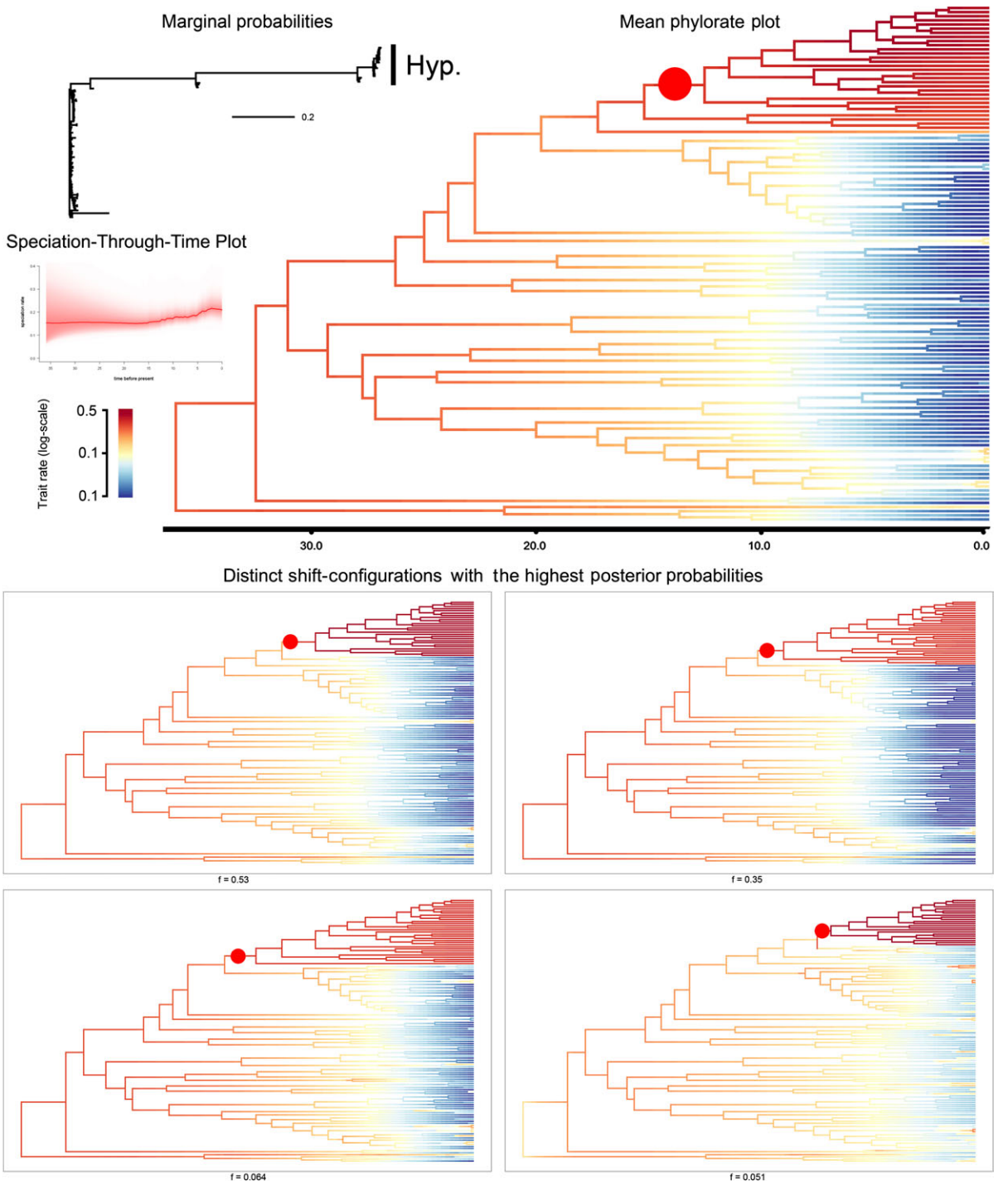

Fig. 2 Phylorate plots showing rates of cladogenesis in the subfamily Hypostominae. Colours along branches denote instantaneous rates (cool colours = slow, warm = fast). The large tree at top depicts the Mean Phylorate Plot, with colours indicating the mean evolutionary rate across all shift configurations sampled during simulation. The circle in this plot indicates the most frequent shift along all sampled trees of the Bayesian analysis. Smaller phylogenies at bottom show the Distinct Shift-Configurations with the Highest Posterior Probabilities. For each distinct shift configuration, the locations of rate shifts are shown as red circles (rate increases). Text labels denote the posterior probability of each shift configuration. The small Marginal Probabilities plot at top left shows rate shifts along all branches, with branch length scaled by the probability that it contains a shift event. The small Speciation-Through-Time Plot at left displays the cumulative speciation rate from the root of the tree to the present computed from the joint posterior density in BAMM. The order of taxa in the phylogeny follows the order in Table S1–S2 and Figs S1–S4 (Supporting information).

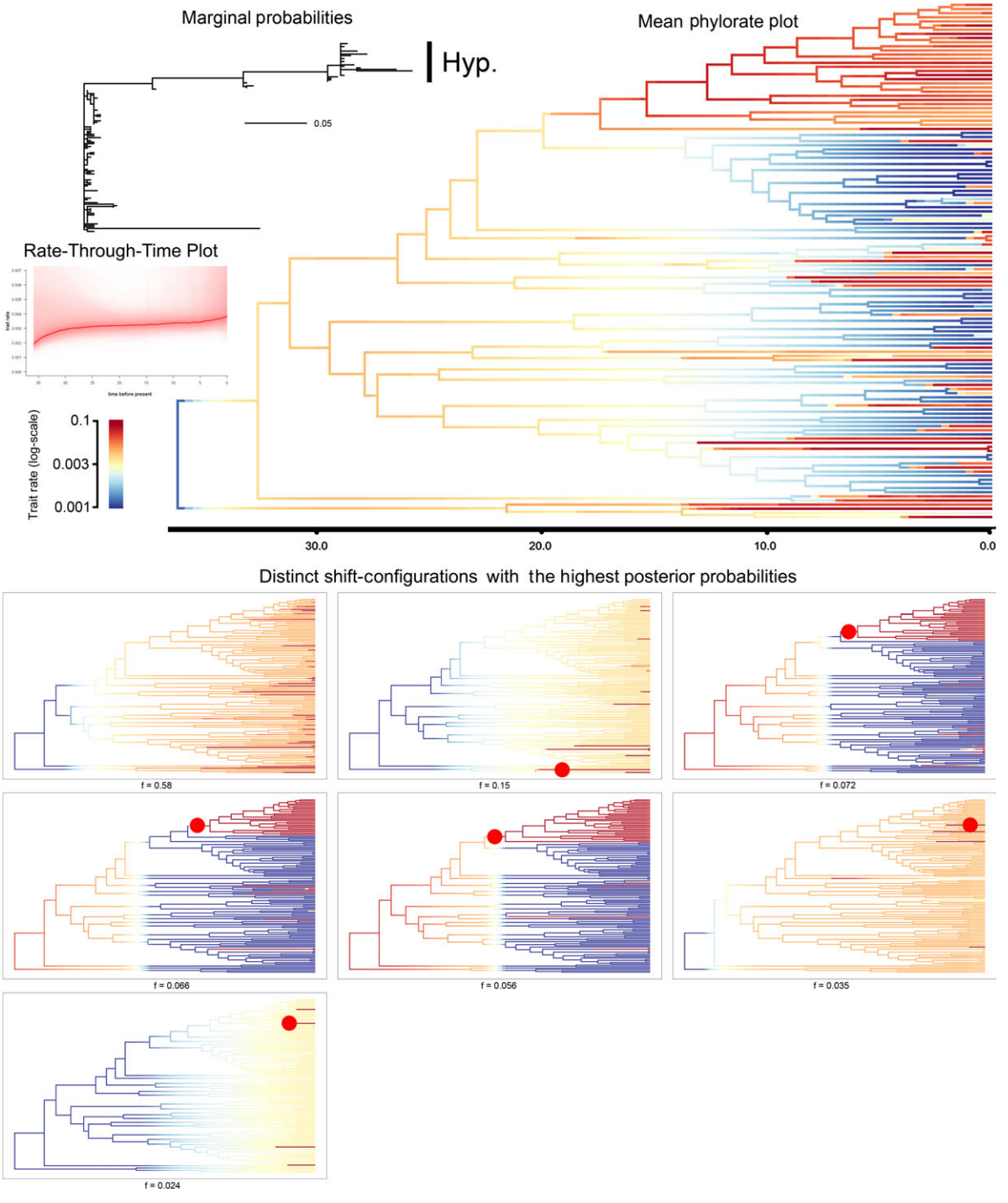

Fig. 3 Phylorate plots showing rates of body shape diversification in the subfamily Hypostominae. Colours along branches denote instantaneous rates (cool colours = slow, warm = fast). The large tree at top depicts the Mean Phylorate Plot, with colours indicating the mean evolutionary rate across all shift configurations sampled during simulation. The circle in this plot indicates the most frequent shift along all sampled trees of the Bayesian analysis. The smaller phylogenies at bottom show the Distinct Shift-Configurations with the Highest Posterior Probabilities. For each distinct shift configuration, the locations of rate shifts are shown as red circles (rate increases). Text labels denote the posterior probability of each shift configuration. The small Marginal Probabilities plot at top left shows rate shifts along all branches, with branch length scaled by the probability that it contains a shift event. The small Rate-Through-Time Plot at left displays the cumulative body shape diversification rate from the root of the tree to the present computed from the joint posterior density in BAMM. The order of taxa in the phylogeny follows the order in Table S1–S2 and Figs S1–S4 (Supporting information).

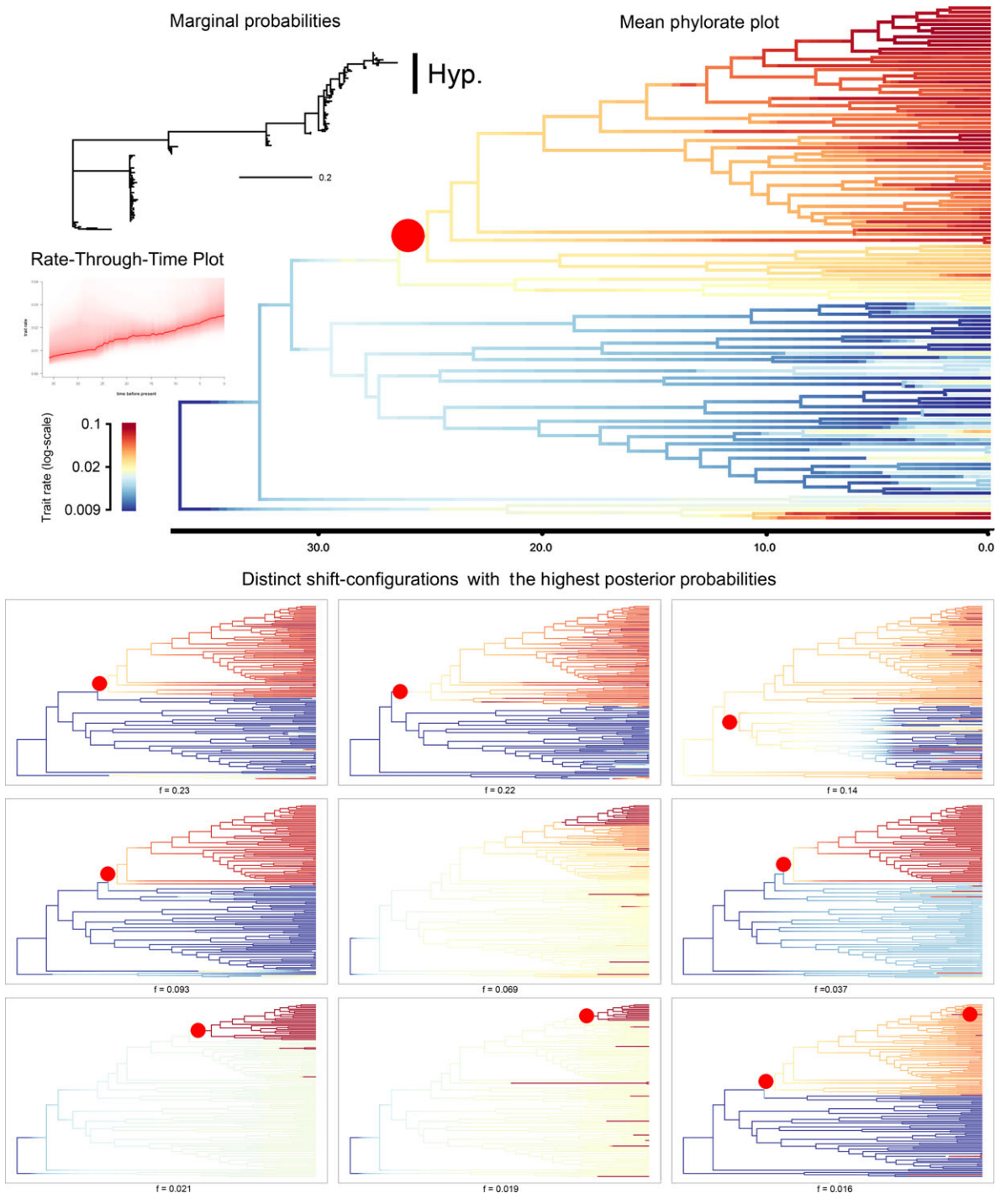

Fig. 4 Phylorate plots showing rates of log maximum body size (MBS) diversification for the subfamily Hypostominae. Colours along branches denote instantaneous rates (cool colours = slow, warm = fast). The large tree at top depicts the Mean Phylorate Plot, with colours indicating the mean evolutionary rate across all shift configurations sampled during simulation. The circle in this phylogeny indicates the most frequent shift along all sampled trees of the Bayesian analysis. The smaller phylogenies at bottom show the Distinct Shift-Configurations with the Highest Posterior Probabilities. For each distinct shift configuration, the locations of rate shifts are shown as red circles (rate increases). Text labels denote the posterior probability of each shift configuration. The small Marginal Probabilities phylogeny at top left shows rate shifts along all branches, with branch length scaled by the probability that it contains a shift event. The small Rate-Through-Time Plot at left displays the cumulative rate of body size diversification from the root of the tree to the present computed from the joint posterior density in BAMM. The order of taxa in the phylogeny follows the order in Table S1–S2 and Figs S1–S4 (Supporting information).

Ancestral habitat estimation

The stochastic character map analysis indicated that ancestors of the genus *Hypostomus* occupied a greater diversity of habits (i.e. channels, riffles, streams, and low and high elevations) than any other Hypostominae lineage (Fig. 5), whereas ancestors of the genus *Ancistrus* occupied the lowest diversity of habitats.

Morphological disparity

The first principal component (PC1) axis explained 27.5% of the variation for Hypostominae species (Fig. 6A) and 22.4% for *Hypostomus* species (Fig. 6B). Characters that loaded strongly on the first principal component for both Hypostominae and the genus *Hypostomus* were anal-fin spine length, mouth width, barbel length, dentary tooth cup length and premaxillary tooth cup length (Table S6). Characters that varied more in *Hypostomus* species than in Hypostominae as a whole were mostly related to the head (e.g. head–eye length, snout length and interorbital width) and fins (e.g. pectoral–spine length, pelvic–spine length, dorsal–pectoral distance, dorsal–spine length, adipose–spine length, dorsal–anal distance; Table S6). Within Hypostominae morphospace, most of the body size/PC1 range occupied by the genus *Hypostomus* overlapped the distributions of other genera (Fig. 6A), whereas within *Hypostomus*, the body size/PC1 area occupied by species from the Paraná River spanned most of the range for the entire genus (Fig. 6B).

Discussion

Macroevolutionary patterns in the suckermouth armored catfish subfamily Hypostominae indicate that, beginning approximately 12.5 Mya (95% HPD: 7.2–19.2 Mya; Fig. 1), the genus *Hypostomus* underwent transcontinental dispersal synchronized with accelerated rates of speciation (Fig. 2) and diversification in body shape (Figs 3, 6 and 7), body size (MBS, Fig. 4) and habitat diversity (Fig. 5). These and other lines of evidence (Cardoso *et al.* 2012) suggest that *Hypostomus*' accelerated diversification was at least partly a response to its repeated invasion of new drainages that likely had reduced predation and competition for food and habitat resources – that is ecological opportunity. Although specific linkages between organismal phenotype and either environment or ecological function remain tenuous at this time, our evidence for monophyly and accelerated diversification in *Hypostomus* suggest that such ecological opportunities promoted an adaptive radiation within a lineage that invaded the upper Paraná River basin in southeastern Brazil approximately 12.5 Mya (95% HPD: 7.2–19.2 Mya; Fig. 1).

The Paraná River is the third largest river in South America by discharge, after the Amazon and Orinoco, yet it is geographically isolated from the hydrologically contiguous Amazon/Orinoco basins to the northwest. It drains southward from highlands of the Brazilian Shield that separate it from the São Francisco drainage to the northeast and the Tocantins drainage to the northwest. Moreover, much of the Paraná basin was dominated by marine conditions as recently as the late Miocene (approx. 10 Mya; Lundberg *et al.* 1998). Due to its geographical remoteness and recent marine incursions, the Paraná River has likely long had a much more depauperate fish fauna than the Amazon. To this day, many of the largest and most distinctive Amazonian piscivores and herbivores are missing from the Paraná, including all osteoglossiform fishes (e.g. *Arapaima* and *Osteoglossum* spp.), the electric eel (*Electrophorus electricus*), the pacu (*Piaractus brachypomus*), as well as the manatee (*Trichechus inunguis*) and freshwater dolphins (*Inia* spp.). The peacock bass genus *Cichla*, which comprises some of the most ubiquitous and iconic piscivorous fishes throughout the Amazon/Orinoco ecoregion, has only recently been introduced to the Paraná by man (Kullander & Ferreira 2006).

The synchronized cladogenesis and geographical, ecological and morphological diversifications of *Hypostomus* across tropical South America, combined with this genus' accelerated diversification upon entering the species-poor Paraná River basin, are highly suggestive of ecological opportunity's influence on this clade's evolution. Historical contributions of ecological opportunity to evolutionary diversifications are often difficult to conclusively demonstrate, especially in large, continental radiations like the Hypostominae (Hughes & Eastwood 2006; Antonelli *et al.* 2009). However, both intrinsic (i.e. organismal) and extrinsic (i.e. environmental) drivers of ecological opportunity can be identified in *Hypostomus*, contributing to a mechanistic understanding of how this genus may have uniquely exploited ecological opportunities historically present in the Paraná River basin.

Intrinsic drivers of accelerated diversification: Evidence for key innovations

Loricariid catfishes are distinguished from all other fishes by having a ventral oral disc, diets consisting largely of algae and detritus, and bodies covered in bony plates and external teeth (i.e. odontodes). *Hypostomus* has no known anatomical traits that might give it a competitive advantage over other loricariids; however, *Hypostomus* species are known to have broad physiological tolerances for diverse diets and habitats. These tolerances may have facilitated their dispersal and been a

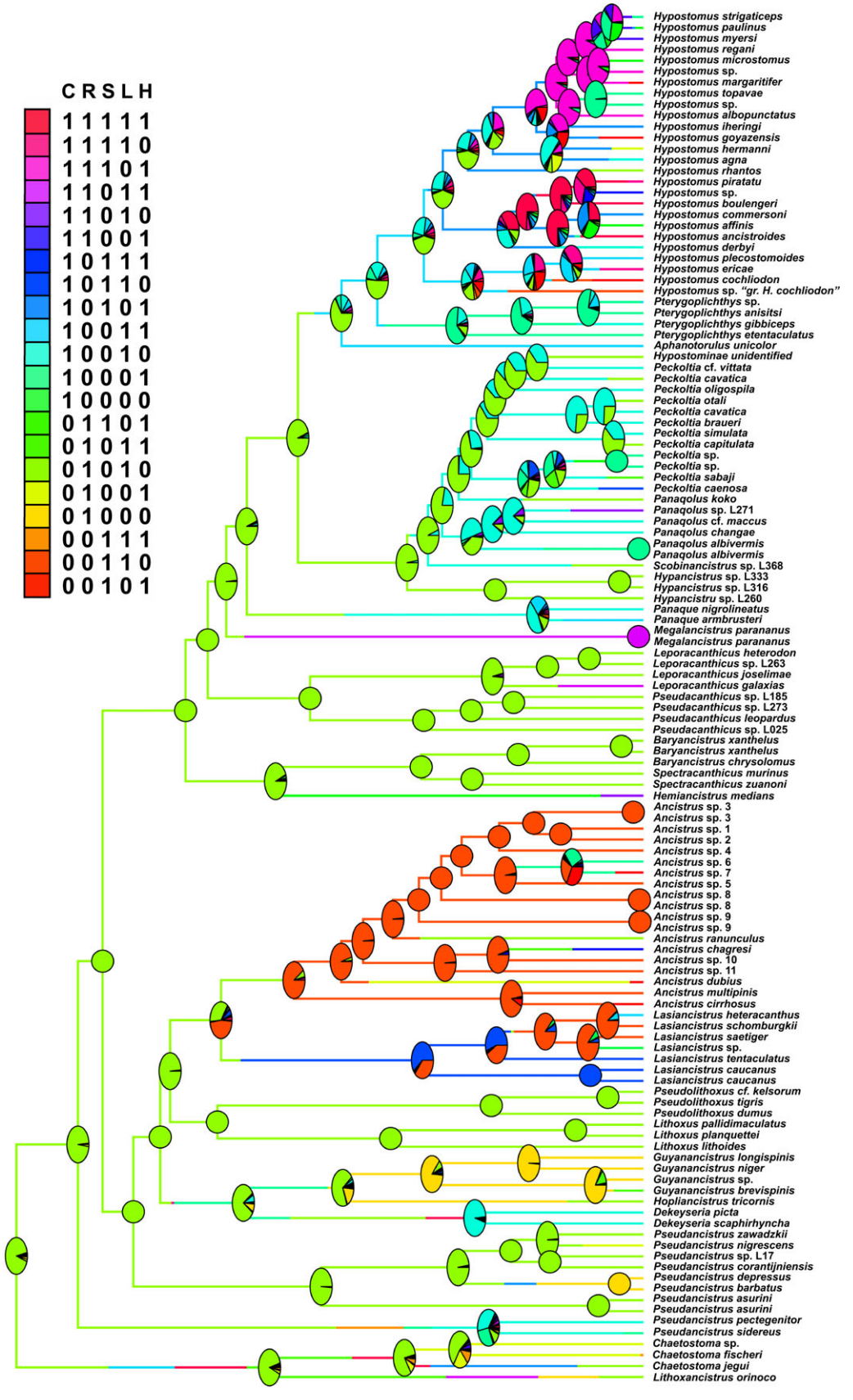

Fig. 5 Ancestral habitat estimates for the subfamily Hypostominae generated using SIMMAP (Bollback 2006). Habitat abbreviations are as follows: C = channel, R = rapids, S = stream, L = low altitude, H = high altitude (habitat characterizations originally proposed by Albert *et al.* 2011). Numbers indicate presence (1) or absence (0) of species in each habitat. Each colour indicates a unique combination of habitats occupied. The genus *Hypostomus*, for example, displays a wider range of unique combinations of habitats than any other genus.

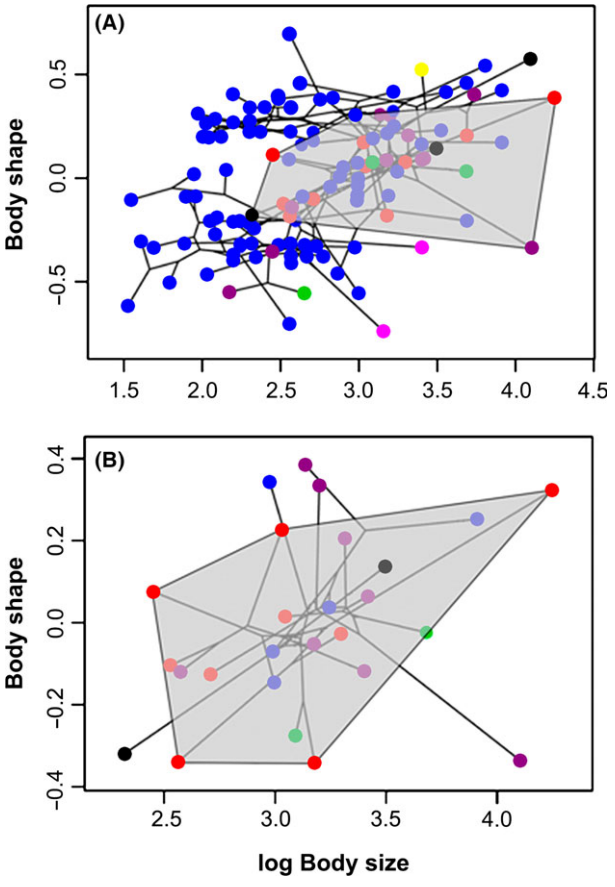

Fig. 6 Phylomorphospace plot for subfamily Hypostominae (A) and genus *Hypostomus* (B). Colours correspond to geographical area classifications used in the ancestral area estimation (Fig. 1). The *y*-axis is the first principal component (PC) from a size-corrected PC analysis of log-normalized linear distances between 31 homologous landmarks distributed across the head, body and fins (following landmarks originally proposed by Armbruster 2003a,b) and the *x*-axis is log maximum body size (MBS). Shaded convex hulls enclose all examined species of *Hypostomus* (A) and all examined species of *Hypostomus* from the Paraná River basin (B).

key to their exceptional invasion and diversification within the Paraná River basin.

In an evolutionary analysis of trophic diversity across 19 sympatric assemblages of loricariid catfishes, Lujan *et al.* (2012) found that *Hypostomus* species tended to specialize on the most nutrient-poor (i.e. protein depauperate or ^{15}N-depleted; Kelly & del Rio 2010) subsets of food resources being ingested and assimilated. Likewise, in a detailed study of resource partitioning among sympatric wood-eating loricariids in northern Peru, Lujan *et al.* (2011) found that a wood-eating member of the genus *Hypostomus* ingested and assimilated the lowest protein (i.e. most ^{15}N-depleted) fraction of submerged woody detritus compared to two unrelated but also wood-eating loricariid genera (i.e. *Panaque* and *Panaqolus*).

The preference or tolerance of *Hypostomus* species for presumably nutrient-poor, low-protein subsets of the food spectrum available to loricariids is complemented by their occupation of a wide range of habitats. Not only are *Hypostomus* ubiquitous and often locally abundant in a wide range of habitats throughout their native range in tropical South America (Fig. 5; Saint-Paul *et al.* 2000), they are also among the most adept of all loricariid genera at invading novel habitats outside their native range. Invasive and often ecologically destructive populations of *Hypostomus* are now established in many drainages around the world, including rivers in Texas (Pound *et al.* 2011), Sri Lanka (Bambaradeniya 2002) and China (Xu *et al.* 2012). *Hypostomus* is one of only two loricariid genera to have broadly established invasive populations outside their native range, the other being the closely related genus *Pterygoplichthys* (Capps & Flecker 2013).

Together, the broad dietary and habitat tolerances of *Hypostomus* species indicate that, although this genus appears to lack key morphological innovations, it likely has key physiological adaptations that facilitate its invasion and survival in environments that are inhospitable to most other loricariids. However, more robust comparative analyses of physiological tolerances and dietary and habitat preferences across the Loricariidae are needed to identify specific traits that allow *Hypostomus* to be so successful.

Extrinsic drivers of accelerated diversification: Evidence for open ecological niches

One of the most distinctive and prominent events in the transcontinental dispersal of *Hypostomus* is the repeated invasion of the Paraná River basin in southeastern Brazil. Results of this and previous (Cardoso *et al.* 2012) studies support at least six independent invasions by ancestral lineages of *Hypostomus* in the upper Paraná (coloured red in Fig. 1; with one large clade occupying

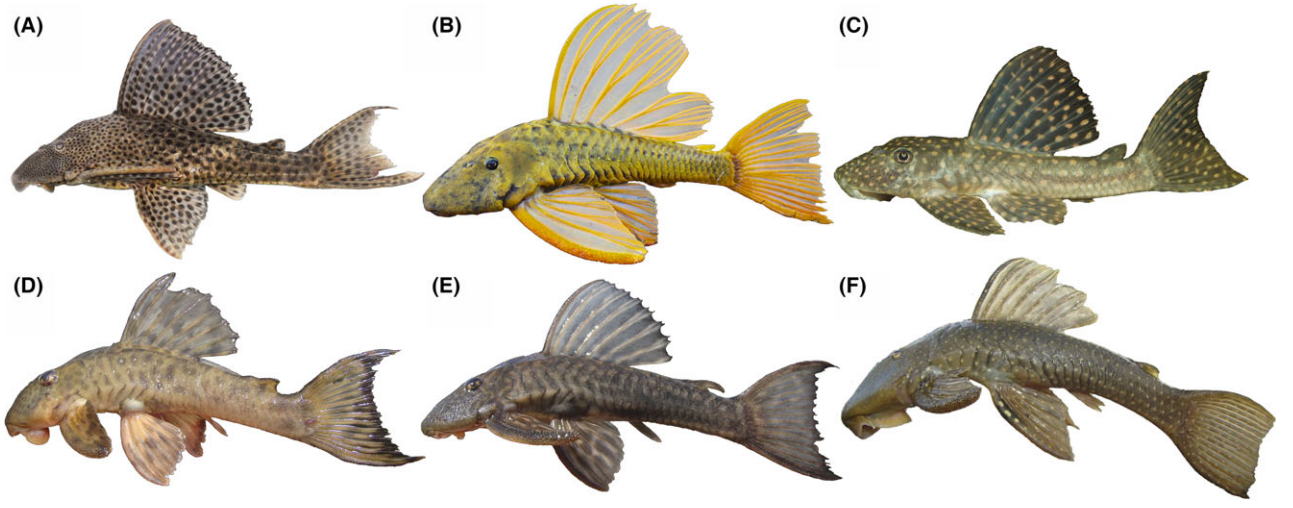

Fig. 7 Variation in colour patterns across the genus *Hypostomus*, with (A) *Hypostomus niceforoi* representing a typical Amazon basin species, and (B) *Hypostomus luteus* (Uruguay basin), (C) *Hypostomus* aff. *roseopunctatus* (Uruguay basin), (D) *Hypostomus hermanni* (rio Tietê basin), (E) *Hypostomus strigaticeps* (rio Tietê basin), and (F) *Hypostomus albopunctatus* (rio Paraná-Paraguay basin) representing diversity throughout the Paraná River basin. Photograph A by NKL, D, E and F by CHZ, B and C by O. Lucanus.

the upper Paraná basin almost exclusively); four invasions into the Paraguay, lower Paraná and Uruguay basins (coloured purple in Fig. 1); and two invasions into Atlantic Coastal drainages (coloured green in Fig. 1). To this day, *Hypostomus* is one of only four Hypostominae genera to have successfully invaded the Paraná River basin, resulting in 52 species, or approximately 37% of all *Hypostomus* species, being present there today. The only other Hypostominae taxa now in the Paraná are 13 species of *Ancistrus*, three species of *Pterygoplichthys* and one species of *Megalancistrus* – each of which occupies a much narrower range of habitats than *Hypostomus* (Fig. 5). The first two of these genera share with *Hypostomus* a preference for or tolerance of ^{15}N-depleted food resources (Lujan *et al.* 2012). *Ancistrus*, though, is phylogenetically distantly related to *Hypostomus*, as is *Megalancistrus* (Lujan *et al.* 2015b).

The only other loricariid genera present in the Paraná basin include two genera of the morphologically distinct whiptail catfish subfamily Loricariinae (*Rineloricaria* with 21 species in Paraná basin and *Harttia* with two species in Paraná basin), and a total of 32 much smaller-bodied species (<10 cm SL) in the subfamily Hypoptopomatinae (*sensu* Lujan *et al.* 2015b; e.g. *Hisonotus*, 17 spp.; *Neoplecostomus*, eight spp.; *Otothyropsis*, four spp.; *Pareiorhina*, two spp.; *Pseudotocinclus*, one sp.; Roxo *et al.* 2012, 2014). There is no fossil or other evidence to suggest that any other loricariid genera occupied this watershed prior to *Hypostomus*.

In contrast to the Paraná Basin, the Amazon and Orinoco basins host diverse assemblages of over 30 Hypostominae genera (Lujan *et al.* 2015b), most of which overlap *Hypostomus* in morphospace (Fig. 6). Given the highly distinctive ecological niche occupied by loricariids as a whole (i.e. benthic, surface-scraping, algivore–detritivores), the very few other similar loricariid species present in the Paraná, and this drainage's distinctive history of biogeographical isolation and marine incursion, it becomes increasingly plausible that when *Hypostomus* first invaded the Paraná River basin, it experienced at least an initial reduction in competitive pressure compared with other parts of its range. Of course, in response to *Hypostomus*' adaptive diversification and consequent saturation of available niches, much of the ecological opportunity historically present in the Paraná is predicted to have been reduced over time (Simpson 1949, 1953).

Linking phenotype to environment and ecological function: Evidence for adaptive radiation in Hypostomus of the Paraná River basin

A hallmark of any adaptive radiation (e.g. African cichlids, Caribbean anoles, Hawaiian silverswords) is tremendous phenotypic diversity as compared with closely related lineages (Rabosky *et al.* 2013; Brawand *et al.* 2014). This disparity is echoed in species of *Hypostomus* from the Paraná River basin, which exhibit as great a range of body shapes and sizes (Fig. 6) and a greater range of colour patterns (Fig. 7) and jaw and tooth morphologies (authors' pers. obs.) than congeners throughout the remainder of the genus' range. Moreover, many morphometric traits that are highly variable across Hypostominae, such as mouth width and premaxillary

and dentary tooth cup lengths (Table S6, Supporting information), are known to be functionally relevant to the distinctive feeding biomechanics of loricariids (Lujan & Armbruster 2012).

Most Amazonian *Hypostomus* exhibit minor variations on a colour pattern consisting of black or dark brown spots on a light brown base colour (Fig. 7A) and exhibit one of only two distinctive ecomorphotypes representative of reciprocally monophyletic subgenera (Lujan *et al.* 2015b). The wood-eater morphotype (subgenus *Cochliodon* or the *Hypostomus cochliodon* group) has a tall head and supraoccipital crest and acute rows of few, large and spoon-shaped teeth. The algivorous morphotype (subgenus *Hypostomus* or the *Hypostomus plecostomus* group) has a depressed head and oblique rows of many, small, villiform teeth. In contrast to bimodal Amazonian diversity, *Hypostomus* in the Paraná basin exhibit a broader and more continuous range of body, jaw and tooth shapes. In addition to both the Amazonian ecomorphotypes, the Paraná basin hosts many distinctive ecomorphotypes not seen elsewhere. These include dorsoventrally depressed species with white polka dots on a dark base colour (e.g. *Hypostomus albopunctatus*, *H. roseopunctatus*; Fig. 7C and F), longitudinally truncate species with angled jaws and few but small, villiform teeth (e.g. *H. peckoltoides*, *H. margaritifer* and *H. microstomus*; not illustrated), and a large-finned species with a stunning yellow-gold base colour (e.g. *H. luteus*; Fig. 7B). Because some of the most distinctive yet rare Paraná basin *Hypostomus* species (e.g. *H. peckoltoides*) were omitted from this study, our results showing an acceleration in body shape diversification (Fig. 3) and broad morphometric diversity (Fig. 6) in Paraná River *Hypostomus* likely underestimate the true diversity of this radiation.

Schluter (2000) proposed four prerequisites to adaptive radiation: (i) common ancestry, (ii) accelerated diversification, (iii) phenotype–environment correlation and (iv) trait utility. Given the monophyly and accelerated diversification in species of *Hypostomus* of the upper Paraná River basin, and a consistent pattern in other loricariid studies of correlation between phenotypic characters examined herein and both environment and ecological function (Casatti & Castro 2006; Lujan & Armbruster 2012; Lujan *et al.* 2012), we find the support for adaptive radiation in *Hypostomus* from the upper Paraná River basin to be compelling. However, specific environmental and functional data from upper Paraná River basin *Hypostomus* are still needed and are the subject of ongoing research by ourselves and collaborators.

Conclusion

There are few clear examples of evolutionary diversification, let alone adaptive radiation, in response to ecological opportunity either in river systems or across continents. The most convincing examples remain those on islands (e.g. birds and lizards, Losos & Ricklefs 2009), in lakes (e.g. African cichlid fishes, Kocher 2004) or at high mountain elevations (e.g. Andean *Lupinus* plants, Hughes & Eastwood 2006), where relatively recent dates of origin for entire ecosystems can be established and rates of speciation and diversification are often striking in an absolute sense. In contrast, the geologic and hydrologic history of the upper Paraná River basin is poorly resolved, and accelerated speciation and diversification rates of *Hypostomus* are striking in a more relative sense. The diversification of *Hypostomus* in the upper Paraná River basin has occurred over a time frame on the order of 10–15 Myr vs. only 100 000 years for African cichlids of Lake Victoria (reference), 1–2 Myr for Andean *Lupinus* (Hughes & Eastwood 2006) and 5 Myr for cichlids of Lake Malawi (reference) and Hawaiian silverswords (Baldwin & Sanderson 1998). Evidence nonetheless remains strong for a single *Hypostomus* lineage having invaded the upper Paraná River basin and experienced accelerated cladogenesis and morphological diversification in response. Moreover, the current and likely historical absence in the Paraná of many competitors and predators that are diverse and abundant in the Amazonian drainages where *Hypostomus* first originated suggests that ecological opportunity played a role in facilitating this accelerated evolution.

Acknowledgements

We are grateful to Ricardo Britzke for helping to collect specimens and to Oliver Lucanus for supplying photographs used in Fig. 7. This research was supported by the Brazilian Agencies FAPESP (Fundação de Amparo à Pesquisa do Estado de São Paulo, proc. 2014/05051–5 and 2015/00691–9 to FFR, and proc. 2012/01622–2 to GSCS), MCT/CNPq (Conselho Nacional de Desenvolvimento Científico e Tecnológico, proc. 310733/2013–8 to CHZ), and Edital Universal CNPq, proc. 441347/2014–2 to FFR. VAT was funded by Programa Nacional de Pós Doutorado – PNPD/CAPES (proc. 16003012001P4). NKL was funded by grant NSF DEB-1257813 (the iXingu Project) and the Canada Department of Fisheries and Oceans.

References

Albert JS, Crampton WGR (2010) The geography and ecology of diversification in Neotropical freshwaters. *Nature Education Knowledge I*, **1**, 3–19.

Albert JS, Petry P, Reis RE (2011) Major biogeographic and phylogenetic patterns. In: *Historical Biogeography of Neotropical Freshwater Fishes* (eds Albert JS, Reis RE), pp. 21–57, University of California Press, Berkeley, Los Angeles.

Alfaro ME, Santini F, Brock C *et al.* (2009) Nine exceptional radiations plus high turnover explain species diversity in jawed vertebrates. *Proceedings of the Natural Academy of Sciences of the USA*, **106**, 13410–13414.

Antonelli A, Nylander JA, Persson C, Sanmartín I (2009) Tracing the impact of the Andean uplift on Neotropical plant evolution. *Proceedings of the Natural Academy of Sciences of the USA*, **106**(24), 9749–9754.

Armbruster JW (2003a) *Peckoltia sabaji*, a new species from the Guyana Shield (Siluriformes: Loricariidae). *Zootaxa*, **344**, 1–12.

Armbruster JW (2003b) The species of the *Hypostomus cochliodon* group (Siluriformes: Loricariidae). *Zootaxa*, **249**, 1–60.

Baldwin BG, Sanderson MJ (1998) Age and rate of diversification of the Hawaiian silversword alliance (Compositae). *Proceedings of the Natural Academy of Sciences of the USA*, **95**, 9402–9406.

Bambaradeniya CNB (2002) The status and implications of invasive alien species in Sri Lanka. *Zoos' Print Journal*, **17**, 930–935.

Bertuzzo E, Muneepeerakul R, Lynch HJ, Fagan WF, Rodriguez-Iturbe I, Rinaldo A (2009) On the geographic range of freshwater fish in river basin. *Water Resources Research*, **45**, 1–11.

Bollback JP (2006) SIMMAP: stochastic character mapping of discrete traits on phylogenies. *BMC Bioinformatics*, **7**, 88.

Boubli JP, Rylands AB, Farias IP, Alfaro ME, Alfaro JWL (2012) *Cebus* phylogenetic relationships: a preliminary reassessment of the diversity of the untufted capuchin monkeys. *American Journal Primatology*, **74**, 381–393.

Brawand D, Wagner CE, Li YI *et al.* (2014) The genomic substrate for adaptive radiation in African cichlid fish. *Nature*, **513**, 375–381.

Capps KA, Flecker AS (2013) Invasive aquarium fish transform ecosystem nutrient dynamics. *Proceedings of the Royal Society of London. Series B, Biological Sciences*, **280**, 20131520.

Cardoso YP, Almirón A, Casciotta J, Aichino D, Lizarralde MS, Montoya-Burgos JI (2012) Origin of species diversity in the catfish genus *Hypostomus* (Siluriformes: Loricariidae) inhabiting the Paraná river basin, with the description of a new species. *Zootaxa*, **3453**, 69–83.

Casatti L, Castro RMC (2006) Testing the ecomorphological hypothesis in a headwater riffles fish assemblage of the rio São Francisco, southeastern Brazil. *Neotropical Ichthyology*, **4**, 203–214.

Chiachio MC, Oliveira C, Montoya-Burgos JI (2008) Molecular systematic and historical biogeography of the armored Neotropical catfishes Hypoptopomatinae and Neoplecostominae (Siluriformes: Loricariidae). *Molecular Phylogenetics and Evolution*, **49**, 606–617.

Cockerell TDA (1925) A fossil fish of the family Callichthyidae. *Science*, **62**, 397–398.

Covain R, Fisch-Muller S (2012) Molecular evidence for the paraphyly of *Pseudancistrus sensu* lato (Siluriformes, Loricariidae), with revalidation of several genera. *Cybium*, **36**, 229–246.

Crowell KL (1962) Reduced interspecific competition among the birds of Bermuda. *Ecology*, **43**, 75–88.

Drummond AJ, Rambaut A (2007) BEAST: Bayesian evolutionary analysis by sampling trees. *BMC Evolutionary Biology*, **7**, 214.

Dryden IL, Mardia KV (1998) *Statistical Shape Analysis*. Wiley, University of Nottingham Press, Les Diablerets, Switzerland.

Edgar RC (2004) Muscle: a multiple sequence alignment method with reduced time and space complexity. *BMC Bioinformatics*, **5**, 1–19.

Ehrlich PR, Raven PH (1964) Butterflies and plants: a study in coevolution. *Evolution*, **18**, 586–608.

Erwin DH (2001) Lessons from the past: biotic recoveries from mass extinctions. *Proceedings of the Natural Academy of Sciences of the USA*, **98**, 5399–5403.

Erwin DH, Valentine JW, Sepkoski JJ Jr (1987) A comparative study of diversification events: the early Paleozoic versus the Mesozoic. *Evolution*, **41**, 1177–1186.

Eschmeyer WN, Fong JD (2015) Species by Family/Subfamily. http://researcharchive.calacademy.org/research/ichthyology/catalog/speciesbyfamily.asp. Accessed February 2016.

Felsenstein J (1985) Confidence limits on phylogenies: an approach using the bootstrap. *Evolution*, **39**, 783–791.

Fricke R, Eschmeyer WN (2015) http://researcharchive.calacademy.org/research/ichthyology/catalog/collections.asp. Accessed February 2016.

Gatz JA (1979) Ecological morphology of freshwater stream fishes. *Tulane Studies in Zoology and Botany*, **21**, 91–124.

Grant CEH, Lowe WH, Fagan WF (2007) Living in the branches: population dynamics and ecological processes in dendritic networks. *Ecology Letters*, **10**, 165–175.

Hallam A, Wignall PB (1997) *Mass Extinctions and Their Aftermath*. Oxford University Press, Oxford, New York.

Hammer O, Harper DAT, Ryan PD (2004) *Past – Palaeontological Statistics, ver. 1.32*. University of Oslo, Oslo.

Hocutt CH, Wiley EO (1986) The zoogeography of North American freshwater fishes.

Houle D, Hughes KA, Hoffmaster DK *et al.* (1994) The effects of spontaneous mutation on quantitative traits. I. Variances and covariances of life history traits. *Genetics*, **138**, 773–785.

Huelsenbeck JP, Ronquist F (2001) MrBayes: Bayesian inference of phylogenetic trees. *Bioinformatics*, **17**, 754–755.

Hughes C, Eastwood R (2006) Island radiation on a continental scale: exceptional rates of plant diversification after uplift of the Andes. *Proceedings of the Natural Academy of Sciences of the USA*, **103**, 10334–10339.

Jobb G, von Haeseler A, Strimmer K (2004) TREEFINDER: a powerful graphical analysis environment for molecular phylogenetics. *BMC Evolutionary Biology*, **4**, 4–18.

Kelly LJ, del Rio CM (2010) The fate of carbon in growing fish: an experimental study of isotopic routing. *Physiological and Biochemical Zoology*, **83**, 473–480.

Kocher TD (2004) Adaptive evolution and explosive speciation: the cichlid fish model. *Nature Reviews Genetics*, **5**, 288–298.

Kocher TD, Thomas WK, Meyer A *et al.* (1989) Dynamics of mitochondrial DNA evolution in animals: amplification and sequencing with conserved primers. *Proceedings of the Natural Academy of Sciences of the USA*, **86**, 6196–6200.

Kullander SO, Ferreira EJG (2006) A review of the South American cichlid genus *Cichla*, with descriptions of nine new species (Teleostei: Cichlidae). *Ichthyological Exploration of Freshwaters*, **17**, 289–398.

Lanfear R, Calcott B, Ho SYW, Guindon S (2012) PartitionFinder: combined selection of partitioning schemes and substitution models for phylogenetic analyses. *Molecular Biology and Evolution*, **29**, 1695–1701.

Lathi DL, Johnson NA, Ajie BC *et al.* (2009) Relaxed selection in the wild. *Trends in Ecology and Evolution*, **24**, 487–496.

Losos BL, de Queiroz K (1997) Evolutionary consequences of ecological release in Caribbean *Anolis* lizards. *Biological Journal of the Linnean Society*, **61**, 459–483.

Losos JB, Ricklefs RE (2009) Adaptation and diversification on islands. *Nature*, **457**, 830–836.

Lujan NK, Armbruster JW (2012) Morphological and functional diversity of the mandible in suckermouth armored catfishes (Siluriformes, Loricariidae). *Journal of Morphology*, **273**, 24–39.

Lujan NK, German DP, Winemiller KO (2011) Do wood grazing fishes partition their niche? Morphological and isotopic evidence for trophic segregation in Neotropical Loricariidae. *Functional Ecology*, **25**, 1327–1338.

Lujan NK, Winemiller KO, Armbruster JW (2012) Trophic diversity in the evolution and community assembly of loricariid catfishes. *BMC Evolutionary Biology*, **12**, 124.

Lujan NK, Meza-Vargas V, Barriga-Salazar R (2015a) Two new *Chaetostoma* group (Loricariidae: Hypostominae) sister genera from opposite sides of the Andes Mountains in Ecuador, with the description of one new species. *Copeia*, **103**, 651–663.

Lujan NK, Armbruster JW, Lovejoy NR, López-Fernández H (2015b) Multilocus molecular phylogeny of the suckermouth armored catfishes (Siluriformes: Loricariidae) with a focus on subfamily Hypostominae. *Molecular Phylogenetics and Evolution*, **82**, 269–288.

Lundberg JG, Marshall LG, Guerrero J, Horton B, Malabarba MCSL, Wesselingh F (1998) The stage for Neotropical fish diversification: A history of tropical South American rivers. In: *Phylogeny and Classification of Neotropical Fishes* (eds Malabarba LR, Reis RE, Vari RP, Lucena ZMS, Lucena CAS), pp. 13–48, Edipucrs, Porto Alegre.

Mace GM, Gittleman JL, Purvis A (2003) Preserving the tree of life. *Science*, **300**, 1707–1709.

Mahler DL, Revell LJ, Glor RE, Losos JB (2010) Ecological opportunity and the rate of morphological evolution in the diversification of Greater Antillean anoles. *Evolution*, **64**, 2731–2745.

Marshall LG, Sempere T, Butler RF (1997) Chronostratigraphy of the mammal-bearing Paleocene of South America. *Journal of South American Earth Sciences*, **10**, 49–70.

Mayden RL (1988) Vicariance biogeography, parsimony, and evolution in north American freshwater Fishes. *Systematic Zoology*, **37**, 329–355.

Meredith RW, Janečka JE, Gatesy J *et al.* (2011) Impacts of the Cretaceous Terrestrial Revolution and KPg extinction on mammal diversification. *Science*, **334**, 521–524.

Miller MA, Pfeiffer W, Schwartz T (2010) Creating the CIPRES Science Gateway for inference of large phylogenetic trees. In *Proceedings of the Gateway Computing Environments Workshop (GCE), New Orleans, LA*, pp. 1–8.

Montoya-Burgos JI, Muller S, Weber C, Pawlowski J (1998) Phylogenetic relationships of the Loricariidae (Siluriformes) based on mitochondrial rRNA gene sequences. In: *Phylogeny and Classification of Neotropical Fishes* (eds Malabarba LR, Reis RE, Vari RP, Lucena ZM, Lucena CAS), pp. 363–375, Edipucrs, Porto Alegre.

Muneepeerakul R, Bertuzzo E, Lynch HJ, Fagan WF, Rinaldo A, Rodriguez-Iturbe I (2008) Neutral metacommunity models predict fish diversity patterns in Mississippi-Missouri basin. *Nature*, **453**, 453–222.

Oliveira C, Avelino GS, Abe KT *et al.* (2011) Phylogenetic relationships within the speciose family Characidae (Teleostei: Ostariophysi: Characiformes) based on multilocus analysis and extensive ingroup sampling. *BMC Evolutionary Biology*, **11**, 275.

Paradis E (2011) Time-dependent speciation and extinction from phylogenies: a least squares approach. *Evolution*, **65**, 661–672.

de Pinna MCC (1993) Higher-level phylogeny of Siluriformes (Teleostei, Ostariophysi), with a new classification of the order. PhD Thesis: City University of New York, New York.

de Pinna MCC (1998) Phylogenetic relationships of Neotropical Siluriformes (Teleostei: Ostariophysi): historical overview and synthesis of hypotheses. In: *Phylogeny and Classification of Neotropical Fishes* (eds Malabarba LR, Reis RE, Vari RP, Lucena CAS, Lucena ZMS), pp. 279–330. Museu de Ciências e Tecnologia da Pontifícia Universidade Católica do Rio Grande do Sul, Porto Alegre.

Pound KL, Nowlin WH, Huffman DG, Bonner TH (2011) Trophic ecology of a nonnative population of suckermouth catfish (*Hypostomus plecostomus*) in a central Texas spring-fed stream. *Environmental Biology of Fishes*, **90**, 277–285.

R Core Team (2014) *R: A Language and Environment for Statistical Computing*. R Foundation for Statistical Computing, Vienna, Austria. http://www.R-project.org/. Accessed Nov 2014.

Rabosky DL (2014) Automatic detection of key innovations, rate shifts, and diversity-dependence on phylogenetic trees. *PLoS ONE*, **9**, e89543.

Rabosky DL, Slater GJ, Alfaro ME (2012) Clade age and species richness are decoupled across the eukaryotic tree of life. *PloS Biology*, **10**, e1001381.

Rabosky DL, Santini F, Eastman J *et al.* (2013) Rates of speciation and morphological evolution are correlated across the largest vertebrate radiation. *Nature Communications*, **4**, 1–8.

Rabosky DL, Donnellan SC, Grundler M, Lovette IJ (2014) Analysis and visualization of complex macroevolutionary dynamics: an example from Australian scincid lizards. *Systematic Biology*, **63**, 610–627.

Rambaut A, Drummond AJ (2007a) Tracerv1.5. http://beast.bio.ed.ac.uk/Tracer. Accessed Nov 2013.

Rambaut A, Drummond AJ (2007b) TreeAnnotator v1.7.5. http://beast.bio.ed.ac.uk/TreeAnnotator. Accessed Nov 2013.

Ree RH, Smith SA (2008) Maximum likelihood inference of geographic range evolution by dispersal, local extinction, and cladogenesis. *Systematic Biology*, **57**, 4–14.

Ree RH, Moore BR, Webb CO, Donoghue MJ (2005) A likelihood framework for inferring the evolution of geographic range on phylogenetic trees. *Evolution*, **59**, 2299–2311.

Revell LJ (2012) Phytools: an R package for phylogenetic comparative biology (and other things). *Methods in Ecology and Evolution*, **3**, 217–223.

Ribbink AJ (1994) Biodiversity and speciation of freshwater fishes with particular reference to African cichlids. In: *Aquatic Ecology: Scale, Pattern and Process* (eds Giller PS, Hildrew AG, Raffaelli DG), pp. 261–288. Blackwell Scientific Publications, Oxford.

Ricklefs RE (2007) Estimating diversification rates from phylogenetic information. *Trends in Ecology and Evolution*, **22**, 601–610.

Ronquist F, Teslenko M, van der Mark P *et al.* (2012) MrBayes 3.2: efficient Bayesian phylogenetic inference and model

choice across a large model space. *Systematic Biology*, **61**, 539–542.
Roughgarden J (1972) Evolution of niche width. *The American Naturalists*, **106**, 683–718.
Roxo FF, Zawadzki CH, Alexandrou MA *et al.* (2012) Evolutionary and biogeographic history of the subfamily Neoplecostominae (Siluriformes: Loricariidae). *Ecology and Evolution*, **2**, 2438–2449.
Roxo FF, Albert JS, Silva GS, Zawadzki CH, Foresti F, Oliveira C (2014) Molecular phylogeny and biogeographic history of the armored neotropical catfish subfamilies Hypoptopomatinae, Neoplecostominae and Otothyrinae (Siluriformes: Loricariidae). *PLoS ONE*, **9**, e105564.
Saint-Paul U, Zuanon J, Villacarta Correa MA, Garcia M, Noemi Fabré N (2000) Fish communities in central Amazonian white- and blackwater floodplains. *Environmental Biology of Fishes*, **57**, 235–250.
Schluter D (2000) *The Ecology of Adaptive Radiation*. Oxford University Press, Oxford.
Sepkoski JJ (1981) A factor analytic description of the Phanerozoic marine fossil record. *Paleobiology*, **7**, 36–53.
Sepkoski JJ (1998) Rates of speciation in the fossil record. *Philosophical Transaction of the Royal Society B Biological Sciences*, **353**, 315–326.
Sepkoski JJ (2002) A compendium of fossil marine animal genera. *Bulletin of American Paleontology*, **36**, 1–560.
Shimodaira H (2002) An approximately unbiased test of phylogenetic tree selection. *Systematic Biology*, **51**, 492–508.
Shimodaira H, Hasegawa M (1999) Multiple comparisons of log-likelihoods with applications to phylogenetic inference. *Molecular Biology and Evolution*, **16**, 1114–1116.
Sidlauskas B (2008) Continuous and arrested morphological diversification in sister clades of characiform fishes: a phylomorphospace approach. *Evolution*, **62**, 3135–3156.
Simpson EH (1949) Measurement of diversity. *Nature*, **163**, 688.
Simpson GG (1953) *The Major Features of Evolution*. Columbia University Press, New York.
Smith GR (1981) Late Cenozoic freshwater fishes of North America. *Annual Review of Ecology and Systematics*, **12**, 163–193.
Soltis PS, Soltis DE, Savolainen V, Crane PR, Barraclough TG (2002) Rate heterogeneity among lineages of tracheophytes: integration of molecular and fossil data and evidence for molecular living fossils. *Proceedings of the National Academy of Sciences of the United States of America*, **99**, 4430–4435.
Sorenson L, Santini F, Alfaro ME (2014) The effect of habitat on modern shark diversification. *Journal of Evolutionary Biology*, **27**, 1536–1548.
Stamatakis A (2006) RAxML-VI-HPC: maximum likelihood-based phylogenetic analyses with thousands of taxa and mixed models. *Bioinformatics*, **22**, 2688–2690.
Stamatakis A, Hoover P, Rougemont J (2008) A rapid bootstrap algorithm for the RAxML web servers. *Systematic Biology*, **57**, 758–771.
Stanley SM (1998) *Macroevolution. Pattern and Process*. The Johns Hopkins University Press, London.
Strimmer K, Rambaut A (2002) Inferring confidence sets of possibly misspecified gene trees. *Proceeding of the Royal Society of London B*, **269**, 137–142.
Sullivan JP, Lundberg JG, Hardman M (2006) A phylogenetic analysis of the major groups of catfishes (Teleostei: Siluriformes) using rag1 and rag2 nuclear gene sequences. *Molecular Phylogenetics and Evolution*, **41**, 636–662.
Tagliacollo VA, Roxo FF, Duke-Sylvester SM, Oliveira C, Albert JS (2015) Biogeographical signature of river capture events in Amazonian lowlands. *Journal of Biogeography*, **42**, 2349–2362.
Travis J (1989) The role of optimizing selection in natural populations. *Annual Review of Ecology, Evolution and Systematics*, **20**, 279–296.
Vari RP (1998) The Curimatidae, a lowland Neotropical fish family (Pisces: Characiformes); distribution, endemism, and phylogenetic biogeography. In: *Proceedings of a Workshop on Neotropical Distribution Patterns* (eds Vanzolini PE, Ronald Heyer W), pp. 343–377. Academia Brasileira de Ciências, Rio de Janeiro.
Venditti C, Meade A, Pagel M (2010) Phylogenies reveal new interpretation of speciation and the Red Queen. *Nature*, **463**, 349–352.
Vrba ES (1980) Evolution, species, and fossils: how does life evolve? *South African Journal of Sciences*, **76**, 61–84.
Winemiller KO (1991) Ecomorphological diversification in lowland freshwater fish assemblages from five biotic regions. *Ecological Monographs*, **61**, 343–365.
Winemiller KO, López-Fernandez H, Taphorn DC, Nico LG, Duque AB (2008) Fish assemblages of Casiquiare River, a corridor and zoogeographical filter for dispersal between the Orinoco and Amazon basin. *Journal of Biogeography*, **35**, 1551–1563.
Xia X, Lemey P (2009) Assessing substitution saturation with DAMBE. In: *The Phylogenetic Handbook: A Practical Approach to DNA and Protein Phylogeny* (eds Lemey P, Salemi M, Vandamme AM), pp. 615–630, Cambridge University Press, Cambridge, UK.
Xia X, Xie Z (2001) DAMBE: data analysis in molecular biology and evolution. *Journal of Heredity*, **92**, 371–373.
Xia X, Xie Z, Salemi M, Chen L, Wang Y (2003) An index of substitution saturation and its application. *Molecular Phylogeny and Evolution*, **26**, 1–7.
Xu H, Qiang S, Genovesi P *et al.* (2012) An inventory of invasive alien species in China. *NeoBiota*, **15**, 1–26.
Yoder JB, Clancey E, Des Roches S *et al.* (2010) Ecological opportunity and the origin of adaptive radiations. *Journal of Evolutionary Biology*, **23**, 1581–1596.

G.S.C.S., F.F.R., N.K.L. and C.O. conceived the ideas. F.F.R. and G.J.C.S. collected the data. F.F.R. and V.A.T. analysed the data. G.S.C.S., F.F.R. and N.K.L. led the writing, and G.S.C.S and C.H.Z. identified all samples.

Data accessibility

DNA sequences: GenBank Accession nos at Table S1 (Supporting information).
Habitat and Ecological information: available at Table S2 (Supporting information).
Morphological characters and time-calibrated tree available at Dryad (doi: 10.5061/dryad.c8q11).

Supporting information

Additional supporting information may be found in the online version of this article.

Table S1. Taxa list, collection vouchers and accessing numbers for sequence data analyzed in the present study (n = 157).

Table S2. Species included in the present study with habitat and Maximum Body Size (MBS) classifications for the internal group.

Table S3. Primers used in the present study to amplify partial sequences of F-reticulon 4, 16S rRNA, cytochrome oxidase subunit I (COI) and cytochrome B (CytB).

Table S4. Nucleotide substitution models for each partition evaluated in the software PartitionFinder (Lanfear *et al*. 2012) and used in the phylogenetic analyses.

Table S5. DEC models tested to estimate distribution ranges inherited by the descending lineages at each node of the tree.

Table S6. Variable loadings in the first Principal Component Analysis (PCA 1) for body shape of combined samples of Hypostominae and for the genus *Hypostomus*.

Table S7. Likelihood-based tests for alternative topologies.

Fig. S1. Tree showing relationships between the Hypostominae, and other loricariid subfamilies (Delturinae, Loricariinae, Otothyrinae, Neoplecostominae, Hypoptopomatinae), Clade A and B) obtained by maximum likelihood and Bayesian analyses.

Fig. S2. Tree showing the relationships among species of the *Ancistrus*, *Lithoxus*, *Dekeyseria* and *Pseudancistrus* clades obtained by maximum likelihood and Bayesian analyses.

Fig. S3. Tree showing relationships among species of the *Hemiancistrus*, *Leporacanthicus*, *Megalancistrus*, *Panaque* and *Peckoltia* clades obtained by maximum likelihood and Bayesian analyses.

Fig. S4. Tree showing relationships among species of the *Hypostomus* clade obtained by maximum likelihood and Bayesian analyses.